(Accepted author manuscript)

Calcium entry via TRPV1 but not ASICs induces neuropeptide release from sensory neurons

Aurélien Boillat, Omar Alijevic and Stephan Kellenberger
Department of Pharmacology and Toxicology, University of Lausanne, 1005 Lausanne, Switzerland

Running title: acid-induced neuropeptide secretion

Correspondence to:
Stephan Kellenberger
Department of Pharmacology and Toxicology
University of Lausanne
Rue du Bugnon 27
CH-1005 Lausanne
Switzerland
Phone ++4121 692 5422
Fax ++4121 692 5355
Stephan.Kellenberger@unil.ch

Abbreviations: ASIC, acid-sensing ion channel; BCTC, 4-(3-Chloro-2-pyridinyl)-*N*-[4-(1,1-dimethylethyl)phenyl]-1-piperazinecarboxamide; Ca_v, voltage-gated calcium channel; CGRP, calcitonin gene-related peptide; DIG, digoxigenin; DRG, dorsal root ganglion; FCS, fetal calf serum; IB4, Isolectin B4; PcTx1, Psalmotoxin 1; ROI, regions of interest; SP, substance P; TRPV1, transient receptor potential vanilloid 1

Abstract

Inflammatory mediators induce neuropeptide release from nociceptive nerve endings and cell bodies, causing increased local blood flow and vascular leakage resulting in edema. Neuropeptide release from sensory neurons depends on an increase in intracellular Ca^{2+} concentration. In this study we investigated the role of two types of pH sensors in acid-induced Ca^{2+} entry and neuropeptide release from dorsal root ganglion (DRG) neurons. The transient receptor potential vanilloid 1 channel (TRPV1) and acid-sensing ion channels (ASICs) are both H^+-activated ion channels present in these neurons, and are therefore potential pH sensors for this process. We demonstrate with *in situ* hybridization and immunocytochemistry that TRPV1 and several ASIC subunits are co-expressed with neuropeptides in DRG neurons. Activation of ASICs and of TRPV1 led to an increase in intracellular Ca^{2+} concentration. While TRPV1 has a high Ca^{2+} permeability and allows direct Ca^{2+} entry when activated, we show here that ASICs of DRG neurons mediate Ca^{2+} entry mostly by depolarization-induced activation of voltage-gated Ca^{2+} channels and only to a small extent via the pore of Ca^{2+}-permeable ASICs. Extracellular acidification led to release of the neuropeptide calcitonin gene-related peptide from DRG neurons. The pH dependence and the pharmacological profile indicated that TRPV1, but not ASICs, induced neuropeptide secretion. In conclusion, this study shows that although both TRPV1 and ASICs mediate Ca^{2+} influx, TRPV1 is the principal sensor for acid-induced neuropeptide secretion from sensory neurons.

Keywords: ASIC, calcitonin gene-related peptide, calcium, proton, sensory neuron, substance P, TRPV1

Introduction

Dorsal root ganglion (DRG) neurons transmit sensory information from the periphery to the CNS. The size of DRG neurons correlates with their function; small-diameter neurons transmit nociceptive information whereas large-diameter neurons are closely related to the transmission of proprioceptive and tactile signals (Harper and Lawson, 1985; Nakamura and Strittmatter, 1996). In addition to their sensory roles, DRG neurons have efferent functions and can release neuropeptides such as substance P (SP) and calcitonin gene-related peptide (CGRP), which regulate inflammatory processes and the blood flow in the microcirculation and can induce and maintain neurogenic inflammation (Steinhoff et al., 2003). Neuropeptide secretion has been observed from peripheral termini and from cell bodies of sensory neurons (Huang and Neher, 1996). The role of neuropeptide secretion from cell bodies is not well understood and may have roles in the modulation of neuronal excitability and provide autocrine and paracrine functions. Since the DRG somata express many of the channels and receptors present in the nerve termini, they are widely used as a sensory neuron model system. Neuropeptide secretion is generally induced by a membrane depolarization and an increase in intracellular Ca^{2+} concentration (Huang and Neher, 1996). A small percentage of vesicle release from DRG somata is Ca^{2+}-independent (Zhang and Zhou, 2002).

Inflammation and ischemia are accompanied by a tissue acidification that activates mainly two types of pH-sensing ion channels in DRG neurons, the transient receptor potential vanilloid 1 (TRPV1) channel and acid-sensing ion channels (ASICs). Activation of these channels may lead to Ca^{2+} entry into the neuron and to neuropeptide secretion. TRPV1 and ASICs have distinct properties and may differently contribute to this process. TRPV1 is activated by noxious warm temperature (>43°C), acidic pH and capsaicin (Caterina et al., 1997; Tominaga et al., 1998). This channel is permeable to Ca^{2+} and Na^{+}. ASICs are homo- or heterotrimeric H^{+}-activated Na^{+} channels (Jasti et al., 2007) that are widely expressed in the central and the peripheral nervous system (Waldmann et al., 1997). Four ASIC genes are known and several of them exist in different splice variants (Wemmie et al., 2006; Wemmie et al., 2013). Among the different ASIC types, only ASIC1a homotrimers and ASIC1a/2b heterotrimers are in addition to Na^{+} also permeable to Ca^{2+} (Bassler et al., 2001; Sherwood et al., 2011; Sutherland et al., 2001; Waldmann et al., 1997). In contrast to TRPV1 which produces sustained currents when the extracellular pH is lowered, ASICs are only transiently activated and desensitize within seconds. The pH required to activate 50% of the channels is in the range of 6 - 6.5 for many ASIC subtypes and ~5 for TRPV1, indicating that TRPV1 requires more acidic conditions for activation than most ASICs (Caterina et al., 1997; Waldmann et al., 1997). There is evidence from studies with knockout mice and pharmacological approaches that both, TRPV1 and ASICs are involved in different forms of inflammation-related pain sensation (Caterina et al., 2000; Patapoutian et al., 2009; Price et al., 2001; Sluka et al., 2009). Since the activation of TRPV1 or ASICs likely increases intracellular Ca^{2+} concentrations either by direct Ca^{2+} entry across these channels or by depolarization-induced activation of voltage-gated Ca^{2+} channels (Ca_Vs), their activation may induce neuropeptide release. Several studies have already demonstrated such a role of TRPV1 in sensory neurons, heart and trachea (Fischer et al., 2003; Kichko and Reeh, 2009; Strecker et al., 2005). It was shown that ASIC3 is not involved in CGRP release from heart or stomach (Auer et al., 2010; Strecker et al., 2005), but a role of other ASIC isoforms in neuropeptide release has not been investigated. Previous observations suggested the existence of DRG neuron subpopulations expressing exclusively Ca^{2+}-permeable ASICs (Poirot et al., 2006). To test whether in these neurons ASICs contribute to neuropeptide release we have first analyzed

in DRG neurons the co-expression of ASIC subunits with the neuropeptides CGRP and SP by using immunocytochemistry and *in situ* hybridization. We measured then the Ca^{2+} entry into DRG neurons due to activation of ASICs and TRPV1 and determined finally the CGRP secretion from DRG neurons after an extracellular acidification. We show that activation of both channel types promotes Ca^{2+} entry and that only TRPV1, but not ASIC activation induces CGRP secretion.

Material and methods

DRG neuron isolation and culture

All experimental procedures on rats were carried out in accordance with the Swiss federal law on animal welfare and had been approved by the committee on animal experimentation of the Canton de Vaud. Rats were killed using CO_2. DRG neurons were prepared as described previously (Poirot et al., 2006). Lumbar DRGs (L1–L6) were removed bilaterally and collected in PBS (in mM, 137 NaCl, 2.7 KCl, 10 Na_2HPO_4, 2 KH_2PO_4, pH 7.4) containing 50 U ml^{-1} penicillin and 50 µg ml^{-1} streptomycin (Invitrogen, Basel, Switzerland). DRGs were then incubated for 2 hours at 37°C in Neurobasal A medium (Invitrogen) complemented with 10% heat-inactivated fetal calf serum (FCS, Invitrogen), 22 mM glucose, and sucrose to adjust the osmolarity to 320 mosmol l^{-1} (named here NeuroA medium), containing 0.125% collagenase type P (Roche, Basel, Switzerland). DRGs were then washed twice with PBS, treated with 0.25% trypsin (Invitrogen) in PBS for 30 min at 37°C, washed with NeuroA and taken up in NeuroA complemented with 50 µg ml^{-1} DNase and soybean trypsin inhibitor (Sigma, Buchs, Switzerland). The ganglia were triturated 4–6 times with a fire-polished Pasteur pipette or a blue micropipette tip to obtain a cell suspension. DRG neurons were plated either on glass coverslips, or in 24-well plates that had previously been coated with a high molecular weight (>300'000 Da) poly-l-lysine (Sigma) solution (0.2 mg ml^{-1}). The neurons were maintained in NeuroA at 37°C, 5% CO_2 and 90% humidity for 3 h. Afterwards, neurons were maintained at 4°C in Leibovitz's L15 medium supplemented with 10% FCS and 5 mM Hepes, pH 7.4, 320 mosmol l^{-1} to prevent changes in protein expression (Blair and Bean, 2002).

Immunocytochemistry

Cells on coverslips were washed three times with PBS and fixed with freshly prepared 4% paraformaldehyde in PBS for 20 min, washed three times in PBS containing 0.5% BSA (protease free, Acros Organics) and permeabilized with 0.4% Triton X-100 (Sigma) in PBS for 10 min. Subsequently, cells were incubated with the first antibody or antibodies (for co-labeling by antibodies of different species) in PBS containing 2% BSA and 0.1% Triton X-100, for two hours at RT. Cells were washed three times in PBS / 0.5% BSA and incubated with secondary antibodies in PBS / 2% BSA / 0.1% Triton X-100 for one hour at RT. Cells were washed three times in PBS / 0.5% BSA. The coverslips were mounted on a glass microscope slide with Vectashield medium (Reactolab, Servion, Switzerland).

The following antibodies were used for immunocytochemistry: NeuN, primary monoclonal mouse antibody (1:500, Merck Millipore, Darmstadt, Germany), secondary antibody coupled with CY5 (1:200, Jackson ImmunoResearch Europe, Suffolk, UK); Neuropeptides, rabbit antibody (SP, 1:1000, BD Biosciences, Allschwil, Switzerland) and (CGRP, 1:1000, Bachem, Bubendorf, Switzerland), secondary antibody coupled to CY3 (1:200, Jackson ImmunoResearch); ion channels, rabbit antibody against ASIC1 (1:500, MTY19 (Wemmie et al., 2003)) rabbit antibody against ASIC2 (1:200, ASIC2 (Gannon et al., 2008)) rabbit antibody against TRPV1 (1:2000, Santa Cruz Biotechnology, Heidelberg, Germany), secondary antibody coupled to FITC (1:200, Jackson ImmunoResearch). None of the commercially available ASIC3 antibodies produced specific staining in our hands. For some experiments two primary antibodies raised in rabbit were used. In these cases, the protocol

was modified in the following way. During the first antibody incubation step, one rabbit antibody was used. This was followed by a 1-hour incubation with a Fab fragment secondary antibody against the first primary antibody (1:200, Jackson ImmunoResearch) to block the epitopes of the primary antibody to avoid any interference with the secondary antibody of the second step (Negoescu et al., 1994). An additional incubation with unconjugated Fab fragments was used to block all the epitopes of the first antibody of the first step (2 hours, 1:100, Jackson ImmunoResearch) (Dou et al., 2004). A second cycle of primary and secondary antibody incubation was then performed, using the second primary and secondary antibodies.

In situ hybridization

Oligonucleotides were labelled with digoxigenin (DIG)-ddUTP with the DIG Oligonucleotide 3'-End Labelling Kit (Roche), following the manufacturer's protocol. The sequences of the anti-sense probes used are indicated in Suppl. Table 1. Sense oligonucleotides were used as negative controls. The protocol of (Kokaia, 2001) was followed for *in situ* hybridization. Cells were rinsed twice in PBS, fixed for 10 min in 4% paraformaldehyde at RT, rinsed twice in PBS and permeabilized for 5 min in PBS / 0.1% Triton X-100 / 5% vanadyl ribonucleoside complex (New England Biolabs, Ipswich, USA). The DIG-labeled probes were applied at a concentration of 5 nM in hybridization buffer (50% (v/v) deionized formamide (Sigma), 4× SSC, 1× Denhardt solution, 1% N-laurylsarcosine (Sigma), 20 mM phosphate pH 7.0, 0.55 mg/ml salmon testes DNA (Sigma), 100 g/l dextran sulphate (Sigma)) and the cover slips were incubated in a humidified chamber at 37°C for 16 to 18 hours. The coverslips were rinsed once with SSC (150 mM NaCl, 15 mM sodium citrate, pH 7.0) at 48°C and incubated three times for 30 min each in SSC at 48°C and then allowed to cool down to RT in 1xSSC. The coverslips were washed twice in binding buffer (150 mM NaCl, 100 mM Tris, pH 7.5) and were incubated for 3 h in a humidified chamber at RT in binding buffer with anti-DIG-fluorescein-conjugated antibody (1:10, Roche), 1% normal sheep serum (Invitrogen) and 0.3% Triton X-100 (Sigma). The coverslips were then washed 4 times in binding buffer, twice in wash buffer (100 mM NaCl, 100 mM Tris, 50 mM $MgCl_2$, pH 9.5), and twice in water.

Microscopy and cell counting

In situ hybridization and immunocytochemistry slides were examined using a confocal microscope (LSM 710, Carl Zeiss, Feldbach, Switzerland) with an EC Plan-Neofluar 40x/1.30 Oil DIC M27 objective and analyzed with ImageJ. The neurons were labeled with an antibody against NeuN to determine the regions of interest (ROI). Each fluorescent region delimited a neuron. The average grey scale value for each other fluorescent dye was then measured in each ROI. For each type of antibody or oligonucleotide, the signal intensity clearly distinguished two sub-populations, corresponding to labeled and non-labeled neurons. A threshold value was chosen that separated optimally the negative from the positive population, and neurons whose signal intensity was above the threshold were counted as positive. The diameter of the neurons was calculated from the area of each ROI.

Calcium imaging

Coated cover slips containing the cells were mounted in the perfusion chamber (Warner Instruments, Hamden, USA) and incubated with 5 µM Fura2-AM in Tyrode solution (in mM, 140 NaCl, 4 KCl, 2 $CaCl_2$, 1 $MgCl_2$, 10 MES, 10 Hepes, 10 glucose) at pH 7.4 for 30 min (CHO cells) or 20 min (neurons) in the dark at 37°C. Experiments were carried out with an inverted microscope (Zeiss Axio Observer). Solutions were changed with the cFlow flux controller (Cell MicroControls, Norfolk, USA) and the Solution Changer Manifold MSC-200 (Bio-Logic, Claix, France) and images were recorded (excitation: 340, 380 nm, emission 520

nm) with a CoolSnap HQ camera (Photometrics, Tucson, USA), using the Metafluor software (Molecular Devices, Sunnyvale, USA). The Na^+-free Tyrode solution contained, in mM, 170 N-methylglucosamine, 4 KCl, 2 $CaCl_2$, 1 $MgCl_2$, 10 MES, 10 HEPES, 10 Glucose, 30 sucrose. For the analysis, the baseline value was subtracted from the peak fluorescence signal.

Substances and chemicals

Stock solutions of the pharmacological substances amiloride, mibefradil, nifedipine (Sigma), PcTx1 (a generous gift from Michel Lazdunski), APETx2 (Smartox, Saint Martin d'Hères, France), Mambalgin-1 (Peptides International, Louisville, USA) and ω-conotoxin MVIIC (Latoxan, Valence, France) were made in water, including 0.3% BSA for the toxins. The stock solution of BCTC (Enzo Life Sciences, Lausen, Switzerland) was made in DMSO. Solutions containing the peptides PcTx1 or ω-conotoxin MVIIC were pre-applied for 60s and then again included in the acidic solution. Mambalgin-1 was pre-applied for 30s but not included in the stimulation solution (Diochot et al., 2012). Mambalgin-1 was tested prior to the CGRP secretion experiments in patch-clamp experiments with human ASIC1a and rat ASIC1b (Suppl. Fig. S1), showing a substantial (~55%) current inhibition and IC50 values that were close to the published values (Diochot et al., 2012). The observed inhibition of ASIC1a is different from the findings of Diochot and colleagues, who had measured a maximally ~80% inhibition of ASIC1a, in contrast to 57 ± 2% in our hands. ASIC1b inhibition by mambalgin-1 was very similar in their study. The observed difference may be due to the different ortholog or the stimulation pH (rat ASIC1a at pH 5.5 in (Diochot et al., 2012), human ASIC1a at pH 6 in the present study). However, these experiments showed that the synthetic mambalgin-1 inhibited at 100 nM ≥ 50% of the pH 6-induced ASIC1 activity.

CGRP secretion assay

Neurons in coated 24-well plates were used ~18h after plating. They were washed with PBS, followed by a washing step with PBS containing protease inhibitors (Leupeptin (1µg/ml), Pepstatin (1µg/ml), Aprotinin (1µg/ml), PMSF (1 mM) (Roche, Rotkreuz, Switzerland) and 0.3 % bovine serum albumin (BSA, protease free, Acros Organics). Protease inhibitors and 0.3 % BSA were included in all solutions used in this assay. Secretion was measured during a 15-min period at 37°C in Tyrode of the same composition as used in the imaging experiments, whose pH had been adjusted to the desired value and which contained pharmacological inhibitors as indicated. It was preceded by a pre-incubation period of 5 min with control or drug-containing Tyrode. The Ca^{2+}-free Tyrode solution contained, in mM, 140 NaCl, 4 KCl, 2$MgCl_2$, 10 MES, 10 Hepes, 10 glucose, 2 EGTA. The KCl Tyrode solution contained, in mM, 70 NaCl, 74 KCl, 2 $CaCl_2$, 1 $MgCl_2$, 10 MES, 10 HEPES, 10 Glucose. After the incubation, the supernatant of each well was transferred into a polyethylene tube (Nunc-Immuno™ Tubes MiniSorp, Fisher Scientific, Wohlen, Switzerland) and kept on ice. Tubes were centrifuged for 10 min at 500 rpm at 4°C. The supernatants were transferred into new polyethylene tubes and then frozen at -80 °C. The cells of each well were incubated for 5 min with 100 µl lysis buffer (150 mM NaCl, 50 mM Tris pH 7.5, 5 mM EDTA, 1% Triton X-100), then harvested. The lysates were transferred to polyethylene tubes, sonicated at 4°C and frozen at -80 °C. They were used to determine the cellular content of CGRP in order to normalize the secretion of each well. The CGRP content of the supernatants and the lysate samples was measured using a rat CGRP enzyme immunoassay kit (SPI-bio, Montigny le Bretonneux, France) according to the manufacturer's recommendations, with the following modifications. The CGRP standard serial dilutions were made in Tyrode, pH 7.4, containing protease inhibitors and 0.3 % BSA. An additional incubation step (O/N, 4°C) was performed between the addition of the samples to the wells and the addition of the tracer.

Statistical analysis
Results are presented as mean ± SEM. A t-test was used for experiments including < 3 groups, and comparison of different groups, if >2 groups were involved, was done by one-way ANOVA followed by Tukey post-hoc test. $P < 0.05$ was considered significant.

Results
ASIC subunits are preferentially expressed in the peptidergic population of small diameter DRG neurons
We analyzed first whether ASICs and TRPV1 were co-expressed with the neuropeptides CGRP or SP in acutely dissociated adult rat DRG neurons. ASIC subunits were visualized with specific antisense probes, while TRPV1, CGRP, SP and the neuronal marker NeuN were detected by specific antibodies (see Materials and methods). Figure 1A illustrates the double labeling of ASIC1a and CGRP. For *in situ* raw data of other ASICs see Suppl. Fig. S2. The presence of NeuN was used to identify neurons. Based on such experiments, the percentage of neurons expressing the channel isoform or the neuropeptide, both or none of them was determined. These experiments were done with neurons of soma diameter ≤ 30 μm. CGRP and SP were detected in approximately 60 % of the neurons (Fig. 1B). ASIC1a mRNA was present in about 60% of small diameter DRG neurons and was co-expressed with CGRP peptide in 43%, and with SP peptide in 49% of small diameter neurons, indicating a large overlap in the expression of ASIC1a and of the neuropeptides (Fig. 1B). ASIC3 mRNA was present in ~50% of the small-diameter neurons. Its degree of co-expression with the neuropeptides was slightly lower than that of ASIC1a. ASIC1b, ASIC2a and ASIC2b were detected in 35-40% of small-diameter neurons. These ASIC subtypes were almost exclusively present in neuropeptide-positive neurons. As a consequence of the lower expression frequency of these ASIC subtypes, approximately 50% of the neuropeptide-positive neurons did not express the ASIC (Fig. 1B). ASIC and also TRPV1 expression was then analyzed by immunocytochemistry. These experiments were carried out on the total population of DRG neurons. TRPV1 was present in about half of the neurons, and was preferentially co-expressed with the neuropeptides (Fig. 1B). The available, tested antibodies for ASIC1 and ASIC2 do not distinguish between splice variants (Gannon et al., 2008; Wemmie et al., 2003). ASIC1 (thus including both splice variants, ASIC1a and ASIC1b) was present in about 50% of the neurons, and was mostly co-expressed with CGRP or SP (Suppl. Figs. S3A-B). ASIC2 was present in ~40% of the neurons; ~80 % of ASIC2-expressing neurons also expressed the neuropeptides, while ~35% of neuropeptide-expressing neurons were ASIC2-negative (Suppl. Fig. S3C), confirming the observations with *in situ* hybridization. In summary, the expression of TRPV1, ASIC1a and ASIC3 in DRG neurons is highly correlated with that of neuropeptides.

Heterologously expressed ASIC1a and TRPV1 mediate acidification-induced Ca^{2+} entry
In a first set of functional experiments on recombinant channels we confirmed with Ca^{2+} imaging that under our experimental conditions both TRPV1 and ASIC1a allow Ca^{2+} entry, and we determined the concentration dependence of their inhibitors for later use (Suppl. Fig. S4A-D). Extracellular acidification induced an increase in intracellular Ca^{2+} concentration in TRPV1- and in ASIC1a-expressing CHO cells. The ASIC inhibitor amiloride and the TRPV1 inhibitor BCTC (4-(3-Chloro-2-pyridinyl)-*N*-[4-(1,1-dimethylethyl)phenyl]-1-piperazinecarboxamide) required concentrations of 500 and 5 μM, respectively, to inhibit 90% of the acidification-induced Ca^{2+} increase.
To determine the Ca^{2+} permeability of ASIC1a, the current-voltage relationship of pH 6-induced currents of ASIC1a was recorded by whole-cell patch-clamp in an extracellular solution that contained as permeant ion either Na^{+} or Ca^{2+} (Suppl. Fig. S4E). From the shift of

the current-voltage relationship the Na^+/Ca^{2+} permeability ratio was calculated as 11.3 ± 2.0 (n=5). In contrast, TRPV1 has a ~10-fold preference for Ca^{2+} with a Na^+/Ca^{2+} permeability ratio of ~0.1 (Caterina et al., 1997).

Amiloride prevents the acid-induced Ca^{2+} entry in a population of DRG neurons

The pharmacological inhibitors were used to determine the relative contribution of TRPV1 and ASICs to acid-induced Ca^{2+} entry in DRG neurons. We classified neurons in Ca^{2+} imaging experiments as partially amiloride-sensitive when 30-70%, and as amiloride-sensitive when >70% of the fluorescence increase at pH 6 was prevented by 500 μM amiloride. The population of amiloride-sensitive neurons, expressing thus almost exclusively ASICs as pH sensors (Fig. 2A & E), comprised 53% of the neurons (Fig. 3E). Twelve percent of the neurons were partially amiloride-sensitive. In these cells, ASICs contribute a part of the Ca^{2+} entry. In 35% of the neurons (Fig. 3E) the pH 5- and pH 6-induced Ca^{2+} entry was not inhibited by 500 μM amiloride (Fig. 2B). In this population amiloride did not affect the amplitude at pH 6, and induced an increase in fluorescence at pH 5, which was however not statistically significant (Fig. 2B & E). Comparison of the relative amplitudes in the absence of amiloride shows that in the amiloride-sensitive and partially -sensitive populations there was no increase in amplitude between pH 6 and pH 5, indicating that pH 6 already fully activated Ca^{2+} entry in these cells. This is consistent with the pH dependence of ASICs. In the amiloride-resistant population, there was a ~40% increase in current amplitude between pH 6 and pH 5, likely reflecting the pH dependence of TRPV1, which requires more acidic pH than ASICs for activation. The fluorescence signal was transient in amiloride-sensitive neurons, returning to basal levels during the extracellular perfusion with the acidic solution. This desensitization was much less pronounced in amiloride-resistant neurons, as shown by the higher ratio between the fluorescence amplitude 20 s after the beginning of the pH 5 stimulation and the peak amplitude (Suppl. Fig. S5, $p<0.01$), consistent with the presence of TRPV1, which does not desensitize (Tominaga et al., 1998). BCTC (5 μM) substantially inhibited the Ca^{2+} entry in half of the amiloride-resistant neurons, indicating that TRPV1 contributed importantly to the Ca^{2+} entry in these neurons (Figs. 2D, 2F and 3E). In amiloride-resistant neurons the desensitization kinetics of the BCTC-resistant Ca^{2+} signal were faster than those of BCTC-sensitive signals. The amplitude at 20s /peak amplitude ratio was at pH 6 0.93 ± 0.04 and 0.60 ± 0.10 (n=4) for the amiloride-resistant BCTC-sensitive and the amiloride- and BCTC-resistant signal, respectively. The nature of the amiloride- and BCTC-resistant Ca^{2+} entry way is not clear. It is however known that K^+ channels, especially some two-pore domain K^+ channels that are also expressed in DRG neurons are inhibited by acidification (Enyedi and Czirjak, 2010; Medhurst et al., 2001). This inhibition would therefore lead to membrane depolarization and possibly to Ca^{2+} entry.

Psalmotoxin 1 identifies neurons expressing Ca^{2+}-permeable ASICs

Psalmotoxin 1 (PcTx1) inhibits homomeric ASIC1a channels at nanomolar concentrations and does not inhibit ASICs formed by other subunits, nor ASIC1a-containing heteromers, with the exception of ASIC1a/2b (Escoubas et al., 2000; Sherwood et al., 2011). PcTx1 is therefore selective for the Ca^{2+}-permeable ASIC isoforms. It was used as a tool to determine the proportion of amiloride-sensitive neurons expressing Ca^{2+}-permeable ASICs. Ten nM PcTx1 inhibited > 70% of the pH 6-induced increase of the intracellular Ca^{2+} concentration in 64% of the amiloride-sensitive neurons, indicating that in these neurons the Ca^{2+} entry was mediated by ASIC1a or ASIC1a/2b (Fig. 3A & D, n=9). This PcTx1-sensitive sub-population accounted for ~30% of the total number of DRG neurons. In the remaining 36% of amiloride-sensitive neurons PcTx1 was ineffective in inhibiting the response to pH 6 (Figs. 3B & D), indicating that in these neurons the Ca^{2+} entry was induced by activation of ASICs other than

ASIC1a and ASIC1a/2b. This result is comparable with a previous study showing that the PcTx1-sensitive current was present in about half of the ASIC-expressing neurons (Poirot et al., 2006). PcTx1 had no effect on amiloride-resistant Ca^{2+} entry (Fig. 3C-D).
Together, the functional experiments indicate the presence of the following neuron populations with regard to acid-induced Ca^{2+} entry, as illustrated in Fig. 3E. In 53% of the neurons ASICs exclusively mediate acid-induced Ca^{2+} entry, in 12% both ASICs and TRPV1 contribute to it, and in the remaining 35%, TRPV1 and other entry ways but no ASICs are involved. Two thirds of the neurons with exclusive ASIC-mediated Ca^{2+} entry are PcTx1-sensitive, expressing therefore ASIC1a homotrimers or ASIC1a/2b heterotrimers.

Inhibitors of voltage-gated Ca^{2+} channels reduce the amplitude of ASIC-mediated Ca^{2+} increase in DRG neurons
TRPV1 as well as ASIC1a and ASIC1a/2b are Ca^{2+}-permeable and can therefore mediate directly the entry of Ca^{2+} when they are activated. The other ASICs and possibly in part also the Ca^{2+}-permeable ASICs may allow Ca^{2+} entry indirectly by membrane depolarization due to their Na^+ inward current, thereby activating Ca_vs. To determine the contribution of Ca_vs, the Ca_v inhibitors Nifedipine (10 μM), Mibefradil (10 μM) and ω-conotoxin MVIIC (300 nM) were used together. Figure 4A illustrates a typical experiment of an amiloride-sensitive neuron, whose pH 6-induced Ca^{2+} entry was strongly decreased by the Ca_v inhibitors. In amiloride-resistant neurons the Ca_v inhibitors did not affect Ca^{2+} entry (Fig. 4B-C). Assuming that the Ca^{2+} entry is mediated in many of these neurons by TRPV1 that has a high Ca^{2+} permeability, less inhibition by the Ca_v blockers would indeed be expected than in amiloride-sensitive neurons.
As another way of testing a direct Ca^{2+} entry versus one mediated by depolarization-activated Ca_vs, Na^+ in the extracellular solution was replaced by the ASIC-impermeant ion N-methylglucosamine to remove the component of the ASIC-mediated depolarization that is due to Na^+ entry. To measure the Ca^{2+} entry via ASICs that are known to display some Ca^{2+} permeability (Sherwood et al., 2011; Waldmann et al., 1997), these experiments were carried out on PcTx1-sensitive neurons. The absence of extracellular Na^+ reduced the fluorescence increase by ~4-fold (Fig. 4D-E), indicating that approximately 25% of the Ca^{2+} entry occurred directly via the ASIC1a or ASIC1a/2b pore.

TRPV1 activation induces CGRP secretion from DRG neurons
To test whether activation of ASICs or TRPV1 leads to neuropeptide secretion, the CGRP concentration in the supernatant of DRG neurons was measured after a 15-min exposure to different pH conditions. The ratio of secreted CGRP/total cellular CGRP content was determined in each secretion experiment, and this ratio, normalized to the corresponding value for the pH 7.4 control condition, is presented in Fig. 5. Extracellular acidification to pH 6 or 5, but not to 6.5 increased the neuronal secretion of CGRP compared to the basal level at pH 7.4 (Fig. 5A). In the absence of extracellular Ca^{2+}, acidification to pH 6 did not increase CGRP secretion (Fig. 5B), confirming that neuropeptide secretion from DRG neurons depends largely on Ca^{2+} entry. Since we have shown in functional experiments that the depolarization due to Na^+ influx plays an important role in the ASIC-mediated Ca^{2+} entry (Fig. 4E) we also tested whether the absence of Na^+ would affect the pH 6-induced CGRP secretion. This was however not the case (Fig. 5B). Amiloride could not be used as ASIC inhibitor in these experiments, since at 500 μM it had a tendency of increasing the CGRP release (data not shown). This increase might be caused by non-specific effects of amiloride during the incubation period that is longer than in Ca^{2+} imaging experiments. In the longer time frame used for these experiments, inhibition of the Na^+/H^+ exchanger or other transporters by amiloride may have ASIC-independent effects on cell function and survival

(Masereel et al., 2003). Alternatively, the recently discovered activation of sustained ASIC3 currents by amiloride (Li et al., 2011; Yagi et al., 2006) might be at the origin of the increased CGRP secretion in the presence of amiloride. This is however less likely, since amiloride activates ASICs only at pH more alkaline than pH 6.5 and we observed the increased CGRP secretion at pH 6 and pH 5 (data not shown). Amiloride had also shown a tendency of increasing Ca^{2+} entry in a population of neurons (Fig. 2B &E). To replace amiloride as ASIC inhibitor we used a combination of peptide toxins. APETx2 inhibits ASIC3 and ASIC3-containing heteromers as well as some voltage-gated Na^{+} channels (Blanchard et al., 2012; Diochot et al., 2003; Peigneur et al., 2012). Mambalgin-1 inhibits ASIC1a, ASIC1b and ASIC1a-containing heteromers (Diochot et al., 2012). The combination of APETx2 and Mambalgin-1 (each at 1 μM) inhibits most of the DRG ASIC currents at pH 6, since ASIC2a and ASIC2a-containing heteromers that do not contain ASIC1a or ASIC3 activate at more acidic pH). The combination of these toxins did however not prevent pH 6-induced CGRP secretion (Fig. 5C). Individual application of these toxins or of PcTx1 did not affect CGRP secretion, excluding a role of the Ca^{2+}-permeable or non-permeable ASICs. In contrast, the TRPV1 inhibitor BCTC (1 μM) significantly reduced the CGRP secretion at pH 6 and 5 (Fig. 5D, $p<0.05$), indicating that TRPV1 is the major sensor involved in acidification-induced CGRP release from DRG neurons. This was further confirmed by the observation that the combination of Ca_v inhibitors did not affect pH 6-induced CGRP secretion (Fig. 5E). Ca_vs contribute to Ca^{2+} entry induced by ASIC activation as shown in Fig. 4, but are certainly less important for Ca^{2+} entry mediated by the highly Ca^{2+}-permeable TRPV1. The Ca_v inhibitors prevented most of the Ca^{2+} entry induced by KCl depolarization, indicating that activation of the DRG Ca_vs can induce neuropeptide secretion, as shown previously in many studies (Huang and Neher, 1996). The KCl-induced depolarization is sustained in contrast to the transient ASIC-induced depolarization.

Discussion

Extracellular acidification induces depolarization and neuropeptide release from DRG neurons. We show that in DRG neurons, TRPV1, ASIC1a and ASIC3 are preferentially co-expressed with the neuropeptides CGRP and SP. The acid-induced Ca^{2+} entry was mediated by ASICs or TRPV1, or both of them together. Acid-induced CGRP secretion depended on extracellular Ca^{2+}. Its pH dependence and pharmacological profile indicate a sensor role for TRPV1 but not ASICs in this process.

Sub-populations of DRG neurons

Our *in situ* hybridization / immunocytochemistry approaches indicate that the two neuropeptides CGRP and SP are present in ~60% of small-diameter DRG neurons and that they are co-expressed in 35-40% of the neurons with TRPV1, ASIC1a or ASIC3. Co-expression of these channels with the neuropeptide is therefore found in 70-100% of neuropeptide-positive neurons. Less correlation with neuropeptide expression was observed for ASIC1b, ASIC2a and ASIC2b. The Ca^{2+} imaging experiments showed that DRG neurons express either functional ASICs or TRPV1, and in a small population of neurons both of them. In approximately 30% of the neurons the PcTx1-sensitive ASIC1a and/or ASIC1a/2b are the exclusive pH sensors.

In most studies investigating co-expression of H^{+}-activated channels and neuropeptides in DRG neurons, the channels were identified by functional analysis. One study measured capsaicin-induced currents in ~60 % and ASIC-like currents in 40% of small-diameter rat DRG neurons (Petruska et al., 2000). We have previously found ASIC currents in ~60 % of small-diameter rat DRG neurons, which were in many neurons co-expressed with TRPV1 (Poirot et al., 2006). In a proportion of these neurons, TRPV1 and the ASICs produced only

small current amplitudes and would probably not be detected by Ca^{2+} imaging or *in situ* hybridization that are less sensitive than patch-clamp. Several studies on rat and mouse DRG neurons showed a preferential ASIC expression in IB4-negative neurons (Dirajlal et al., 2003; Liu et al., 2004; Poirot et al., 2006). In mouse, IB4-negative DRG neurons express almost exclusively neuropeptides, while this negative correlation is much weaker in rat (Barabas et al., 2012; Price and Flores, 2007).
PcTx1-sensitive currents were found only in 5% of rat DRG neurons in one study (Deval et al., 2008), and in ~30% of DRG neurons in our previous study (Poirot et al., 2006). Recently it was shown that PcTx1 inhibits not only ASIC1a homotrimers as initially thought, but also ASIC1a/2b heterotrimeric channels (Sherwood et al., 2011). The same study also showed that zinc exerts a stronger inhibition on ASIC1a than on ASIC1a/2b. In DRG neurons a strong inhibition by zinc of PcTx1-sensitive currents was observed (Poirot et al., 2006), suggesting that a substantial proportion of the PcTx1-sensitive DRG neurons express ASIC1a homotrimers. One study analyzed the expression of TRPV1 and of individual ASIC subunits by *in situ* hybridization in rat DRG sections (Ugawa et al., 2005). In the cited study, ASIC1a and ASIC1b were mostly detected in distinct neurons, and were in a small percentage of neurons co-expressed with other ASIC subunits. ASIC subunits were expressed in 10-35% of neurons, thus at a lower frequency than in other studies. TRPV1 was present in ~40% of neurons, and in many of them together with ASIC1a or ASIC3. In conclusion, although our *in situ* hybridization analysis rather suggests a high degree of co-expression of different ASIC subunits within single neurons, it is consistent with the possible existence of a sub-population of neurons expressing a high proportion of ASIC1a homotrimers, identified with PcTx1 in the Ca^{2+} imaging experiments and in previous functional studies.

Pathway of acid-induced Ca^{2+} entry into DRG neurons
TRPV1 has a high Ca^{2+} permeability, whereas most ASICs are Ca^{2+}-impermeable and only ASIC1a and ASIC1a/2b are to some extent Ca^{2+} permeable (Bassler et al., 2001; Sherwood et al., 2011; Sutherland et al., 2001; Waldmann et al., 1997). Therefore it is expected that ASICs allow Ca^{2+} entry in part by direct Ca^{2+} conductance and in part by depolarization-induced activation of Ca_vs. Several studies demonstrated the Ca^{2+} permeability of recombinant ASIC1a, however the estimates of the Na^+ /Ca^{2+} permeability ratio varied between 1.8 and 18.5 (Bassler et al., 2001; Sherwood et al., 2011; Sutherland et al., 2001; Waldmann et al., 1997; Yermolaieva et al., 2004). Thus, there is solid evidence for a Ca^{2+} permeability of the recombinant ASIC1a in spite of a recent study that challenged these findings by proposing the Ca^{2+} entry through ASIC1a channels to be negligible (Samways et al., 2009). In Ca^{2+} imaging with neurons, a clear distinction between the direct and the indirect ASIC-mediated Ca^{2+} would require pharmacological blockade of Ca_vs, or ion substitution and has not been reported so far. A study measuring simultaneously ASIC currents and increases in intracellular Ca^{2+} concentrations in DRG neurons found Ca^{2+} increases that closely matched the ASIC current kinetics, but could not completely exclude an indirect Ca^{2+} entry (Jiang et al., 2006). By measuring the current-voltage relationship of ASIC currents in PC12 cells, a Ca^{2+} permeability was demonstrated (Chu et al., 2002). We show here, by using Ca_v inhibitors and ion substitution experiments that the ASIC-mediated Ca^{2+} influx in DRG neurons is largely Ca_v-dependent. Even in neurons whose H^+-induced Ca^{2+} influx was inhibited by PcTx1 and thus mediated by Ca^{2+}-permeable ASICs, only ~25% of the Ca^{2+} influx occurred directly via the ASICs. The high Ca^{2+} permeability of TRPV1 is well documented, and further confirmed by our observation that Ca_v inhibitors did not affect Ca^{2+} entry in amiloride-resistant neurons.

Calcium entry via TRPV1, but not ASICs induces CGRP secretion

We show that acidification induces CGRP secretion that largely depends on the presence of extracellular Ca^{2+}, indicating that Ca^{2+}-independent secretion mechanisms account at most for a small proportion of CGRP secretion. We observed CGRP release from DRG neurons by acidification to pH 5 and 6, but not pH 6.5. Many ASIC subtypes display substantial activity at pH 6.5, while the pH dependence of TRPV1 is shifted by approximately one pH unit to more acidic values. The pH dependence and the pharmacological profile of the CGRP release showed that TRPV1, but not ASICs mediate the acid-induced CGRP secretion. As mentioned in the introduction, TRPV1-mediated neuropeptide secretion has been shown in several studies from different tissues (Fischer et al., 2003; Kichko and Reeh, 2009; Strecker et al., 2005). Given the clear evidence for co-expression of ASICs and neuropeptides, and ASIC-mediated Ca^{2+} entry, what are the possible reasons for the incapacity of ASICs to induce neuropeptide secretion? Close sub-cellular co-localization may be required for linking the Ca^{2+} entry to the neuropeptide release, and this may be different between ASICs/Ca_vs and TRPV1. We show that Ca_v activation by KCl-induced depolarization induces CGRP secretion. Electrical stimulation was shown to induce neuropeptide secretion via Ca_v activation in skin-nerve preparations, indicating together that Ca_vs are well positioned for this purpose (Kress et al., 1999). In the cited study the electrical stimulation was strong and lasted for several min. Likely, the Ca^{2+} entry needs to be sufficiently intense and long lasting to induce neuropeptide secretion. Although we did not determine the absolute intracellular Ca^{2+} concentrations reached in Ca^{2+} imaging experiments, the comparison of the amplitude of fluorescence changes mediated by amiloride-sensitive and -resistant pathways showed no obvious difference between these two groups. We observed however with ASIC-mediated Ca^{2+} entry after the peak a fast decline in intracellular Ca^{2+} concentration that was not observed in amiloride-resistant cells. It is likely that during a sustained acidification the ASIC-mediated Ca^{2+} entry may be limited by the channel desensitization.

In conclusion, we have examined the contribution of TRPV1 and of ASICs to acid-induced neuropeptide secretion from DRG neurons. While we confirm a role of TRPV1 in this process, we show that ASICs, although co-expressed with neuropeptides and capable of mediating Ca^{2+} entry do not induce CGRP secretion.

Acknowledgments

We thank Sophie Roy for expert technical assistance. We thank Heather Drummond for providing ASIC2 antibodies, John Wemmie for ASIC1 antibodies and Michel Lazdunski for PcTx1. We are grateful to Eric Grouzmann for help with the neuropeptide secretion assay. We thank Miguel van Bemmelen, Olivier Poirot and Gaetano Bonifacio for their comments on a previous version of the manuscript. This work was supported by the Swiss National Science Foundation grant 310030_135542 to SK.

References

Auer, J., Reeh, P.W., Fischer, M.J., 2010. Acid-induced CGRP release from the stomach does not depend on TRPV1 or ASIC3. Neurogastroenterol. Motil. 22, 680-687.

Barabas, M.E., Kossyreva, E.A., Stucky, C.L., 2012. TRPA1 is functionally expressed primarily by IB4-binding, non-peptidergic mouse and rat sensory neurons. PloS one 7, e47988.

Bassler, E.L., Ngo-Anh, T.J., Geisler, H.S., Ruppersberg, J.P., Grunder, S., 2001. Molecular and functional characterization of acid-sensing ion channel (ASIC) 1b. J. Biol. Chem. 276, 33782-33787.

Blair, N.T., Bean, B.P., 2002. Roles of tetrodotoxin (TTX)-sensitive Na^+ current, TTX-resistant Na^+ current, and Ca^{2+} current in the action potentials of nociceptive sensory neurons. J. Neurosci. 22, 10277-10290.

Blanchard, M.G., Rash, L.D., Kellenberger, S., 2012. Inhibition of voltage-gated Na(+) currents in sensory neurones by the sea anemone toxin APETx2. Br J Pharmacol 165, 2167-2177.

Caterina, M.J., Leffler, A., Malmberg, A.B., Martin, W.J., Trafton, J., Petersen-Zeitz, K.R., Koltzenburg, M., Basbaum, A.I., Julius, D., 2000. Impaired nociception and pain sensation in mice lacking the capsaicin receptor. Science 288, 306-313.

Caterina, M.J., Schumacher, M.A., Tominaga, M., Rosen, T.A., Levine, J.D., Julius, D., 1997. The capsaicin receptor - a heat-activated ion channel in the pain pathway. Nature 389, 816-824.

Chu, X.P., Miesch, J., Johnson, M., Root, L., Zhu, X.M., Chen, D., Simon, R.P., Xiong, Z.G., 2002. Proton-gated channels in PC12 cells. J. Neurophysiol. 87, 2555-2561.

Deval, E., Noel, J., Lay, N., Alloui, A., Diochot, S., Friend, V., Jodar, M., Lazdunski, M., Lingueglia, E., 2008. ASIC3, a sensor of acidic and primary inflammatory pain. EMBO J 27, 3047-3055.

Diochot, S., Baron, A., Salinas, M., Douguet, D., Scarzello, S., Dabert-Gay, A.S., Debayle, D., Friend, V., Alloui, A., Lazdunski, M., Lingueglia, E., 2012. Black mamba venom peptides target acid-sensing ion channels to abolish pain. Nature 490, 552-555.

Diochot, S., Loret, E., Bruhn, T., Beress, L., Lazdunski, M., 2003. APETx1, a new toxin from the sea anemone Anthopleura elegantissima, blocks voltage-gated human ether-a-go-go-related gene potassium channels. Mol Pharmacol 64, 59-69.

Dirajlal, S., Pauers, L.E., Stucky, C.L., 2003. Differential response properties of IB4-positive and -negative unmyelinated sensory neurons to protons and capsaicin. J. Neurophysiol. 89, 513-524.

Dou, H., Xu, J., Wang, Z., Smith, A.N., Soleimani, M., Karet, F.E., Greinwald, J.H., Jr., Choo, D., 2004. Co-expression of pendrin, vacuolar H^+-ATPase alpha4-subunit and carbonic anhydrase II in epithelial cells of the murine endolymphatic sac. J. Histochem. Cytochem. 52, 1377-1384.

Enyedi, P., Czirjak, G., 2010. Molecular background of leak K^+ currents: two-pore domain potassium channels. Physiol Rev 90, 559-605.

Escoubas, P., DeWeille, J.R., Lecoq, A., Diochot, S., Waldmann, R., Champigny, G., Moinier, D., Ménez, A., Lazdunski, M., 2000. Isolation of a tarantula toxin specific for a class of proton-gated Na^+ channels. J. Biol. Chem. 275, 25116-25121.

Fischer, M.J., Reeh, P.W., Sauer, S.K., 2003. Proton-induced calcitonin gene-related peptide release from rat sciatic nerve axons, in vitro, involving TRPV1. Eur J Neurosci 18, 803-810.

Gannon, K.P., Vanlandingham, L.G., Jernigan, N.L., Grifoni, S.C., Hamilton, G., Drummond, H.A., 2008. Impaired pressure-induced constriction in mouse middle cerebral arteries of ASIC2 knockout mice. Am. J. Physiol. Heart Circ. Physiol. 294, H1793-1803.

Harper, A.A., Lawson, S.N., 1985. Conduction velocity is related to morphological cell type in rat dorsal root ganglion neurones. J Physiol 359, 31-46.

Huang, L.Y.M., Neher, E., 1996. Ca^{2+}-Dependent Exocytosis in the Somata of Dorsal Root Ganglion Neurons. Neuron 17, 135-145.

Jasti, J., Furukawa, H., Gonzales, E.B., Gouaux, E., 2007. Structure of acid-sensing ion channel 1 at 1.9 A resolution and low pH. Nature 449, 316-323.

Jiang, N., Rau, K.K., Johnson, R.D., Cooper, B.Y., 2006. Proton sensitivity Ca^{2+} permeability and molecular basis of acid-sensing ion channels expressed in glabrous and hairy skin afferents. J. Neurophysiol. 95, 2466-2478.

Kichko, T.I., Reeh, P.W., 2009. TRPV1 controls acid- and heat-induced calcitonin gene-related peptide release and sensitization by bradykinin in the isolated mouse trachea. Eur J Neurosci 29, 1896-1904.
Kokaia, Z., 2001. In Situ Hybridization Histochemistry. Current Protocols in Toxicology 2, 2.7.1–2.7.13.
Kress, M., Guthmann, C., Averbeck, B., Reeh, P.W., 1999. Calcitonin gene-related peptide and prostaglandin E2 but not substance P release induced by antidromic nerve stimulation from rat skin in vitro. Neuroscience 89, 303-310.
Li, W.G., Yu, Y., Huang, C., Cao, H., Xu, T.L., 2011. The nonproton ligand sensing domain is required for paradoxical stimulation of ASIC3 channels by amiloride. J Biol Chem 286, 42635-42646.
Liu, M., Willmott, N.J., Michael, G.J., Priestley, J.V., 2004. Differential pH and capsaicin responses of Griffonia simplicifolia IB4 (IB4)-positive and IB4-negative small sensory neurons. Neuroscience 127, 659-672.
Masereel, B., Pochet, L., Laeckmann, D., 2003. An overview of inhibitors of Na+/H+ exchanger. Eur. J. Med. Chem. 38, 547-554.
Medhurst, A.D., Rennie, G., Chapman, C.G., Meadows, H., Duckworth, M.D., Kelsell, R.E., Gloger, II, Pangalos, M.N., 2001. Distribution analysis of human two pore domain potassium channels in tissues of the central nervous system and periphery. Mol. Brain Res. 86, 101-114.
Nakamura, F., Strittmatter, S.M., 1996. P2Y1 purinergic receptors in sensory neurons: contribution to touch-induced impulse generation. Proc Natl Acad Sci U S A 93, 10465-10470.
Negoescu, A., Labat-Moleur, F., Lorimier, P., Lamarcq, L., Guillermet, C., Chambaz, E., Brambilla, E., 1994. F(ab) secondary antibodies: a general method for double immunolabeling with primary antisera from the same species. Efficiency control by chemiluminescence. J. Histochem. Cytochem. 42, 433-437.
Patapoutian, A., Tate, S., Woolf, C.J., 2009. Transient receptor potential channels: targeting pain at the source. Nat Rev Drug Discov 8, 55-68.
Peigneur, S., Beress, L., Moller, C., Mari, F., Forssmann, W.G., Tytgat, J., 2012. A natural point mutation changes both target selectivity and mechanism of action of sea anemone toxins. FASEB J 26, 5141-5151.
Petruska, J.C., Napaporn, J., Johnson, R.D., Gu, J.G.G., Cooper, B.Y., 2000. Subclassified acutely dissociated cells of rat DRG: Histochemistry and patterns of capsaicin-, proton-, and ATP-activated currents. J. Neurophysiol. 84, 2365-2379.
Poirot, O., Berta, T., Decosterd, I., Kellenberger, S., 2006. Distinct ASIC currents are expressed in rat putative nociceptors and are modulated by nerve injury. J Physiol 576, 215-234.
Price, M.P., McIlwrath, S.L., Xie, J., Cheng, C., Qiao, J., Tarr, D.E., Sluka, K.A., Brennan, T.J., Lewin, G.R., Welsh, M.J., 2001. The DRASIC cation channel contributes to the detection of cutaneous touch and acid stimuli in mice. Neuron 32, 1071-1083.
Price, T.J., Flores, C.M., 2007. Critical evaluation of the colocalization between calcitonin gene-related peptide, substance P, transient receptor potential vanilloid subfamily type 1 immunoreactivities, and isolectin B4 binding in primary afferent neurons of the rat and mouse. J Pain 8, 263-272.
Samways, D.S., Harkins, A.B., Egan, T.M., 2009. Native and recombinant ASIC1a receptors conduct negligible Ca^{2+} entry. Cell Calcium 45, 319-325.
Sherwood, T.W., Lee, K.G., Gormley, M.G., Askwith, C.C., 2011. Heteromeric acid-sensing ion channels (ASICs) composed of ASIC2b and ASIC1a display novel channel

properties and contribute to acidosis-induced neuronal death. J Neurosci 31, 9723-9734.
Sluka, K.A., Winter, O.C., Wemmie, J.A., 2009. Acid-sensing ion channels: A new target for pain and CNS diseases. Curr. Opin. Drug Discov. Devel. 12, 693-704.
Steinhoff, M., Stander, S., Seeliger, S., Ansel, J.C., Schmelz, M., Luger, T., 2003. Modern aspects of cutaneous neurogenic inflammation. Arch. Dermatol. 139, 1479-1488.
Strecker, T., Messlinger, K., Weyand, M., Reeh, P.W., 2005. Role of different proton-sensitive channels in releasing calcitonin gene-related peptide from isolated hearts of mutant mice. Cardiovasc. Res. 65, 405-410.
Sutherland, S.P., Benson, C.J., Adelman, J.P., McCleskey, E.W., 2001. Acid-sensing ion channel 3 matches the acid-gated current in cardiac ischemia-sensing neurons. Proc. Natl. Acad. Sci. USA 98, 711-716.
Tominaga, M., Caterina, M.J., Malmberg, A.B., Rosen, T.A., Gilbert, H., Skinner, K., Raumann, B.E., Basbaum, A.I., Julius, D., 1998. The cloned capsaicin receptor integrates multiple pain-producing stimuli. Neuron 21, 531-543.
Ugawa, S., Ueda, T., Yamamura, H., Shimada, S., 2005. In situ hybridization evidence for the coexistence of ASIC and TRPV1 within rat single sensory neurons. Mol. Brain Res. 136, 125-133.
Waldmann, R., Champigny, G., Bassilana, F., Heurteaux, C., Lazdunski, M., 1997. A proton-gated cation channel involved in acid-sensing. Nature 386, 173-177.
Wemmie, J.A., Askwith, C.C., Lamani, E., Cassell, M.D., Freeman, J.H., Welsh, M.J., 2003. Acid-sensing ion channel 1 is localized in brain regions with high synaptic density and contributes to fear conditioning. J. Neurosci. 23, 5496-5502.
Wemmie, J.A., Price, M.P., Welsh, M.J., 2006. Acid-sensing ion channels: advances, questions and therapeutic opportunities. Trends Neurosci 29, 578-586.
Wemmie, J.A., Taugher, R.J., Kreple, C.J., 2013. Acid-sensing ion channels in pain and disease. Nature reviews Neurosci. 14, 461-471.
Yagi, J., Wenk, H.N., Naves, L.A., McCleskey, E.W., 2006. Sustained currents through ASIC3 ion channels at the modest pH changes that occur during myocardial ischemia. Circ Res 99, 501-509.
Yermolaieva, O., Leonard, A.S., Schnizier, M.K., Abboud, F.M., Welsh, M.J., 2004. Extracellular acidosis increases neuronal cell calcium by activating acid-sensing ion channel 1a. Proc. Natl. Acad. Sci. U. S. A. 101, 6752-6757.
Zhang, C., Zhou, Z., 2002. Ca(2+)-independent but voltage-dependent secretion in mammalian dorsal root ganglion neurons. Nat Neurosci 5, 425-430.

Figure Legends

Fig. 1. Preferential co-expression of TRPV1, ASIC1a and ASIC3 with neuropeptides in small diameter DRG neurons. A. Analysis of ASIC1a and CGRP expression in DRG neurons. Shown is anti-NeuN antibody staining (purple), ASIC1a antisense probe staining (green), and anti-CGRP antibody staining (red), and a merge of ASIC1a and CGRP staining; scale bar, 100 μm. **B**. Pie charts showing the proportion of neurons expressing ASIC1a, -1b, -2a, -2b, -3 or TRPV1 and either CGRP or SP, in DRG neurons. ASIC expression (green) was determined by *in situ* hybridization, neuropeptide (CGRP in red, SP in red with white dots) and TRPV1 expression (blue) by immunocytochemistry. Labeling of 58-357 neurons from 1-4 animals was measured per analysis type.

Fig. 2. Amiloride inhibits the acid-induced Ca^{2+} entry in a population of DRG neurons. Ca^{2+} imaging from DRG neurons. **A-D**. Representative experiments from an amiloride-sensitive neuron (**A**), an amiloride-resistant neuron (**B**), an amiloride- and BCTC-resistant

neuron (**C**) and an amiloride-resistant, BCTC-sensitive neuron (**D**). Note that **C** and **D** are shown on a different time scale and that the last pH 6 application is longer than the previous applications. **E**. Summary of experiments with amiloride (500 μM), the $F_{340/380}$ ratio is normalized to this ratio at pH 5 control, n = 4-5 for each group. Neurons were classified as "partially amiloride-sensitive" if amiloride prevented 30-70% of the increase in intracellular Ca^{2+} concentration, and "amiloride-sensitive" if inhibition was > 70%. **F**. Effect of 5 μM BCTC on pH 6-induced Ca^{2+} entry in amiloride-resistant neurons, n=4 for each group. For C and D, *, $p < 0.05$, **, $p<0.01$ compared to the respective condition without inhibitor (ANOVA, followed by Tukey post-hoc test).

Fig. 3. PcTx1 inhibits Ca^{2+}-permeable ASICs in a sub-population of amiloride-sensitive neurons. Ca^{2+} imaging from DRG neurons. Representative experimental traces of pH 6-induced intracellular Ca^{2+} concentration increase are shown for **A**, a neuron inhibited by amiloride and PcTx1, **B**, a neuron inhibited by amiloride but not PcTx1 and **C**, a neuron resistant to both inhibitors. **D**, Summary of PcTx1 experiments. The $F_{340/380}$ ratio is normalized to that of the pH 6 control, n = 5-9 for each group; inhibitor concentrations were 500 μM amiloride and 10 nM PcTx1. PcTx1 was pre-applied for 1 min and co-applied with the pH 6 solution. *, $p < 0.05$ and, **, $p < 0.01$ compared to pH 6 control in direct comparison (paired ANOVA and Tukey post-hoc test). The $F_{340/380}$ ratio in the presence of PcTx1 was different between the three groups, and the $F_{340/380}$ ratio in the presence of amiloride was different between the amiloride-sensitive and –resistant groups (ANOVA and Tukey post-hoc test, $p<0.05$, not indicated in the figure). **E**, Pie chart summarizing the proportions of the different populations and sub-populations of neurons, based on the functional experiments (Figs. 2 and 3, n=42).

Fig. 4. Opening of voltage-gated Ca^{2+} channels is involved in ASIC-mediated Ca^{2+} entry. Representative experimental traces of pH 6-induced intracellular Ca^{2+} concentration increase are shown for **A**, an amiloride-sensitive neuron partially inhibited by the combination of Ca_v inhibitors Nifedipine (10 μM), Mibefradil (10 μM) and ω-conotoxin MVIIC (300 nM) and **B**, an amiloride-resistant neuron whose Ca^{2+} entry was not affected by the Ca_v inhibitors. **C**, Summary of the data with Ca_v inhibitors. The $F_{340/380}$ ratio is normalized to the pH 6 control, n=10. **D**, Representative experiment and **E**, summary of experiments with pH 6-induced Ca^{2+} entry in PcTx1-sensitive (10 nM) neurons with normal and Na^+-free Tyrode solution, n=3-4. PcTx1 was pre-applied for 1 min and co-applied with the pH 6 solution. For **C** and **E**, *, $p<0.05$ and ***, $p<0.001$, compared to control pH 6-induced Ca^{2+} entry (Paired ANOVA and Tukey post-hoc test).

Fig. 5. Extracellular acidification promotes CGRP secretion from DRG neurons via the activation of TRPV1. Secretion was measured for 15 min at 37°C. The amount of secreted CGRP is expressed as % of the total CGRP content of the cells, normalized to the condition at pH 7.4. **A**, pH dependence of CGRP secretion. **B**, Dependence on the presence of extracellular Ca^{2+} or Na^+. **C**, Effect of ASIC antagonists. The concentrations used for the experiments were 10 nM PcTx1, 1μM mambalgin-1, 1μM APETx2. **D**, Effect of 1 μM BCTC. **E**, Effect of Ca_v inhibitors; nifedipine (10 μM), mibefradil (10 μM) and ω-conotoxin MVIIC (300 nM) were used together.**F**, depolarization-induced CGRP secretion by 70 mM KCl (pH 7.4). All drugs were pre-applied for 5 min and were co-applied during the secretion experiment; n = 7-28 (A), n = 4-6 (B), n = 3-9 (C), n = 6-12 (D), n = 4-12 (E), n = 6-7 (F). *, **, ***, different from pH 7.4 control, $p < 0.05$, $p < 0.01$ and $p < 0.001$, respectively; #, different from the corresponding control condition at the same pH ($p < 0.05$); one-way ANOVA followed by Tukey post-hoc test, carried out before normalization to pH 7.4 control.

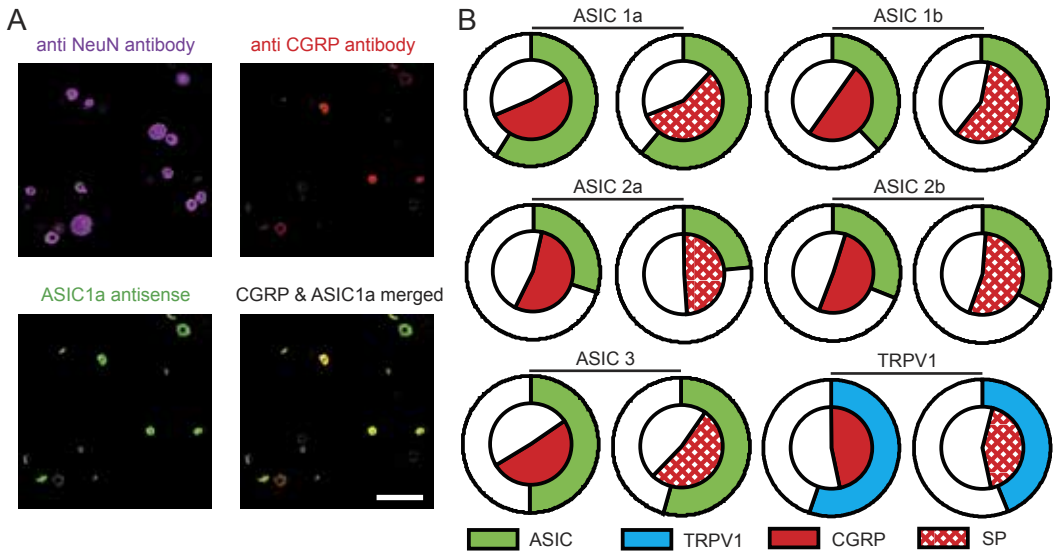

Figure 1, Boillat et al.

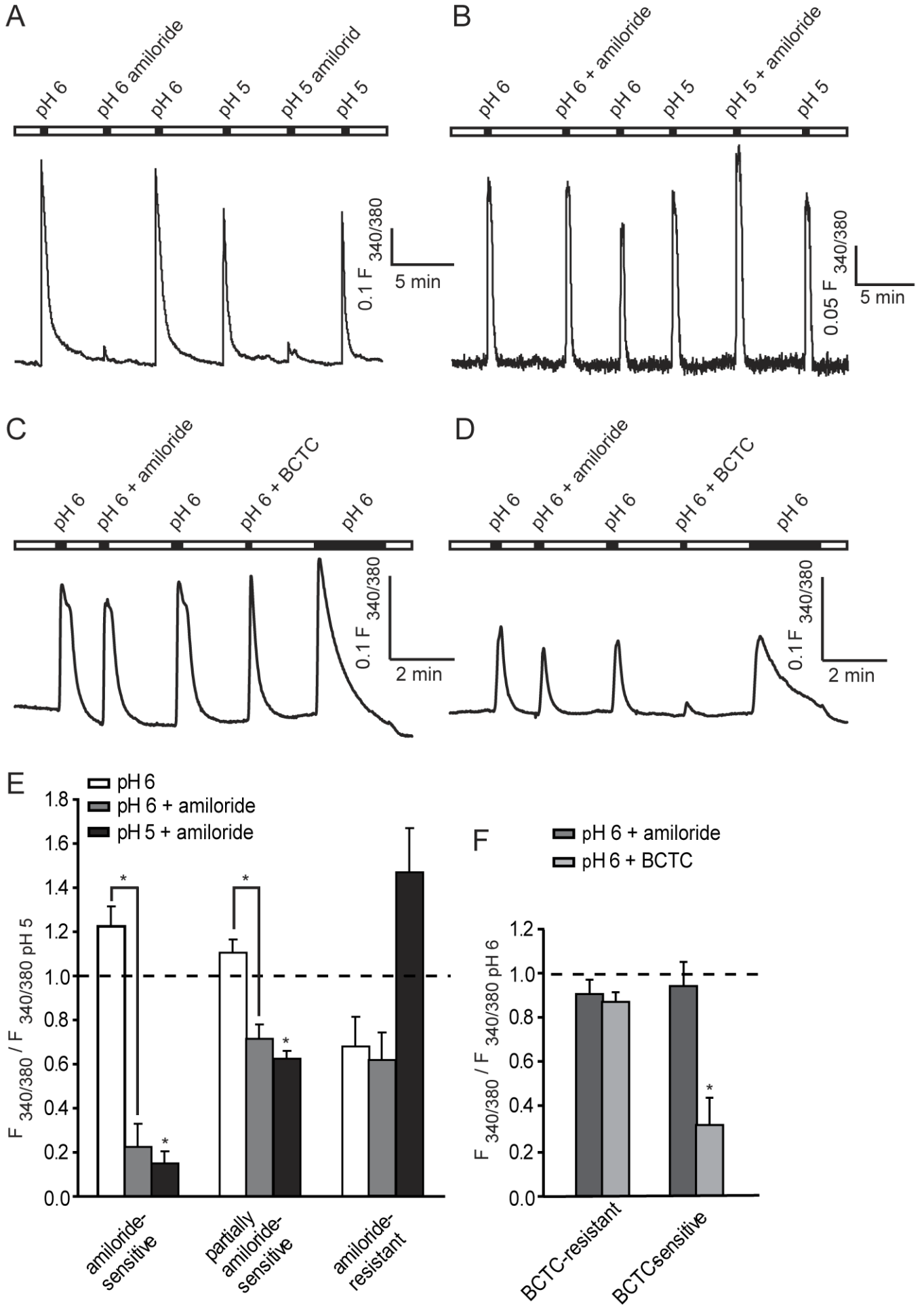

Figure 2, Boillat et al.

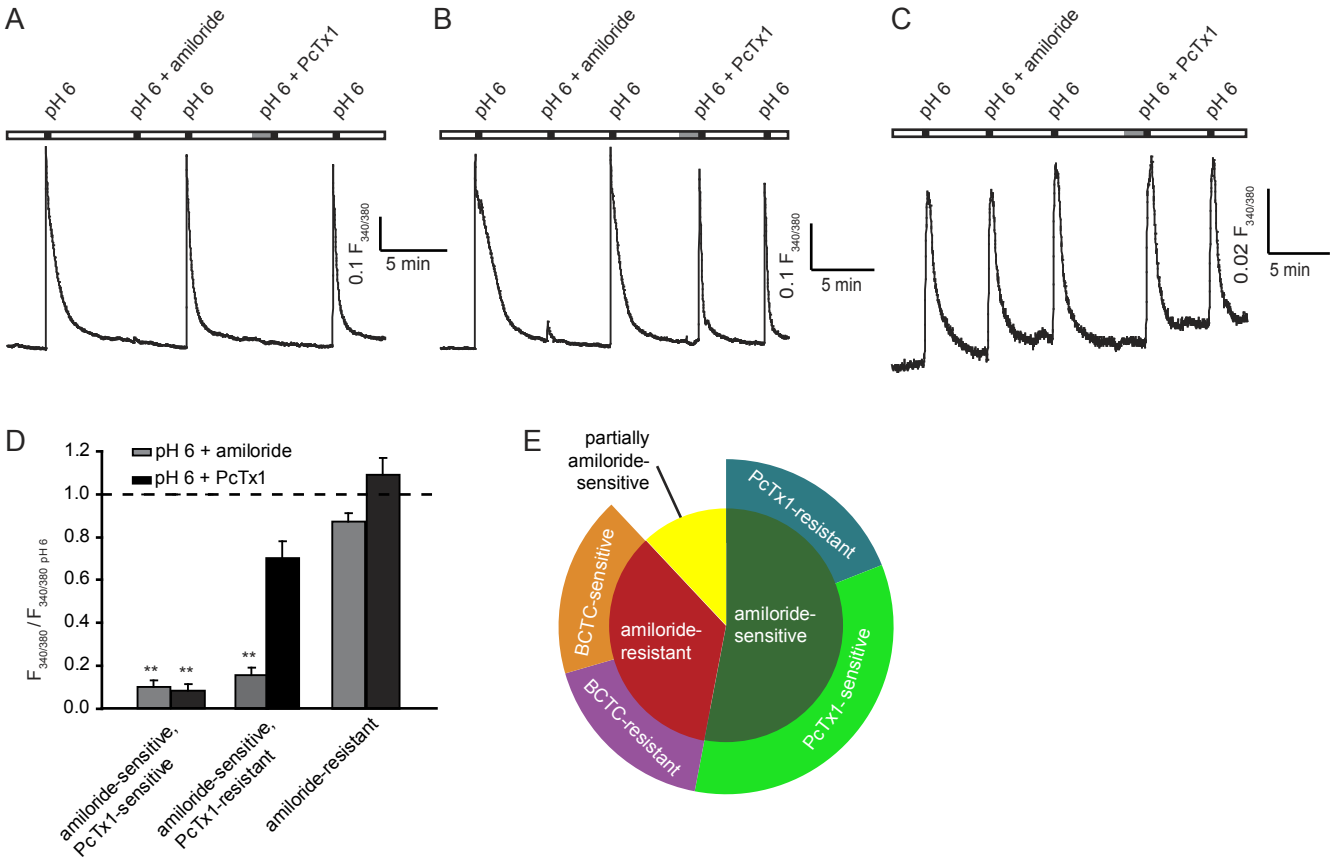

Figure 3, Boillat et al.

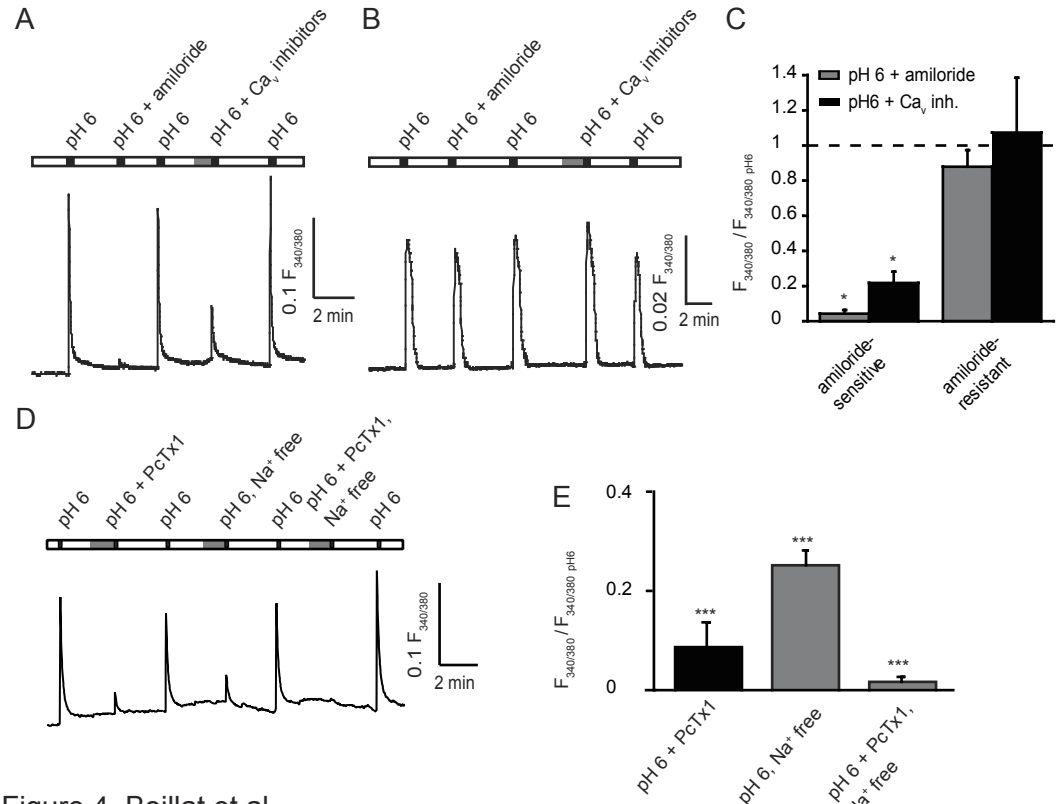

Figure 4, Boillat et al.

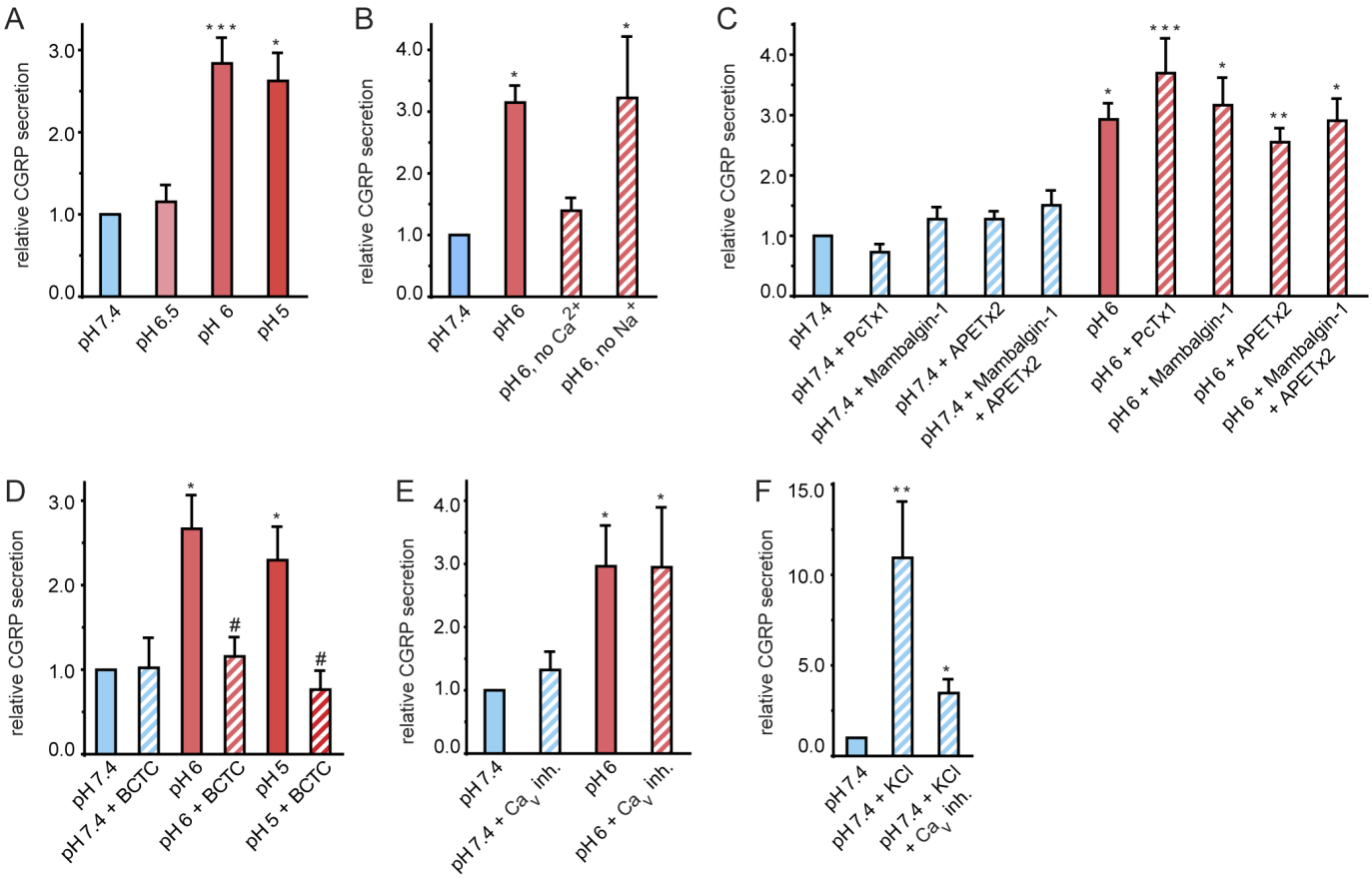

Figure 5, Boillat et al.